On the Swelling of Bicontinuous Lyotropic Mesophases

Johan Engblom, S. Hyde

J. Phys. II France 5 (1995) 171–190 JANUARY 1995, PAGE 171

Classification
Physics Abstracts
61.30 — 61.10 — 68.10

On the Swelling of Bicontinuous Lyotropic Mesophases (*)

Johan Engblom (**) and S. T. Hyde

Applied Mathematics Dept., Research School of Physical Sciences, Australian National University, Canberra, 0200, Australia

(Received 6 June 1994, accepted in final form 19 September 1994)

Abstract. — The swelling of sponge-like bicontinuous mesophases of bilayers of surfactant (or lipid) in water as a function of dilution is analyzed. Analytic formulae for the swelling are derived assuming (i) constant aggregate thickness and (ii) fixed surface area per surfactant molecule at an imaginary surface located within the bilayer. Approximate swelling laws are derived for bicontinuous films and compared with swelling behaviour of disconnected sheet-like, rod-like and globular aggregates. It is shown that sponge-like "oil-in-water" bicontinuous aggregates can be readily distinguished from rods, sheets or globules in surfactant/lipid aggregates; the morphologies of aggregates of reversed curvature ("water-in-oil") are less easily deduced from swelling data. Accurate scaling laws for (ordered or disordered) symmetric and asymmetric sponges, sheets, rods and globules are compared with experimental data of bicontinuous cubic phases in the binary glycerol monooleate - water system and the pseudo-binary didodecyl dimethyl ammonium bromide - cyclohexane - water system as well as some data within dilute sponge-like phases. In the latter cases, scattering data as a function of composition admit identification of symmetric and asymmetric sponge phases.

Introduction

This paper addresses the issue of swelling in lyotropic mesophases, particularly bicontinuous mesophases, which consist of sponge-like aggregates. The work is motivated by recent reports of accurate swelling measurements of bicontinuous cubic phases [1-3]. Given the availability of accurate structural data as a function of composition, we are perhaps now in a position to move beyond structural description and explore the physics of these phases, such as stability and the location of neutral surfaces [4].

Bicontinuous phases are made of mixtures of surfactant (or lipid) and water. The most celebrated cases are the cubic phases [5-7] and L_3 ("sponge") phases [8-10]. The morphology

(*) While we wrote this paper, we received sad news of the death of Dr Krister Fontell in Lund. Both of us have been touched by Krister's humility and gentleness, and helped by his wealth of knowledge of surfactant self-assembly. This paper is humbly dedicated to his memory.

(**) *Permanent address*: Dept. of Food Technology, Chemical Center, Lund University, Box 124, S-22100 Lund, Sweden.

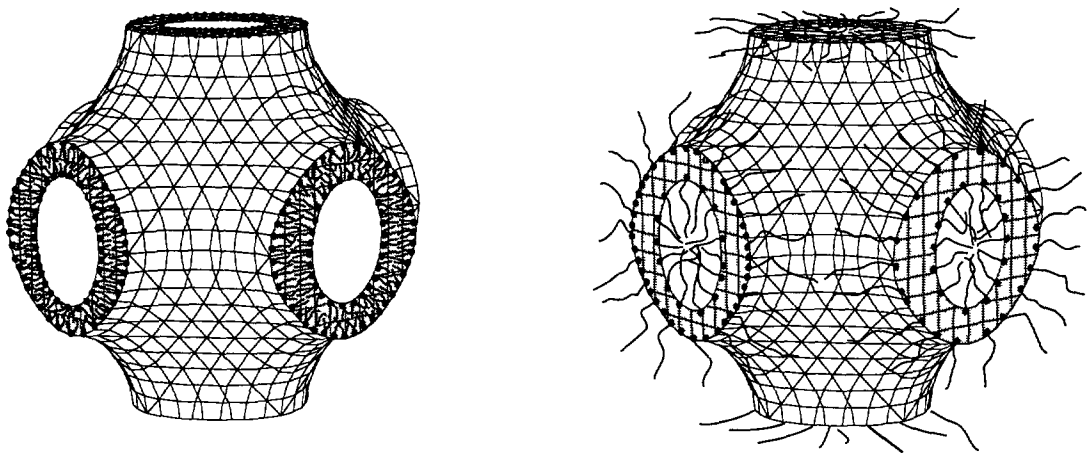

Fig. 1 — Schematic picture of one possible bicontinuous cubic phase, of symmetry Im3m and genus three per unit cell (related to the P-surface) (Left) A reversed cubic phase (V_2), with the surfactant bilayer centred on the P-surface (Right) A direct cubic phase (V_1), with the water film centred on the P-surface.

of sponge phases is probably variable, although in some systems they can be well modelled as random sponge-like bilayers immersed in water or oil continua. The sponges may be both "symmetric" or "asymmetric", depending on the mean curvature at the centre of the bilayer. Symmetric sponge phases are characterized by zero mean curvature at the mid-surface of the bilayer, so that both constituent monolayers are curved equally; asymmetric phases have nonzero mean curvature at the mid-surface of the bilayer. In the case of cubic phases, the mesophase consists of a single-sheeted, hyperbolic surfactant or lipid bilayer immersed in interpenetrating water continua ("reversed" phases, V_2 bicontinuous cubic phases) or a polar film in hydrophobic continua ("normal" phases, V_1 phases). In reversed crystalline mesophases made up of a monodisperse surfactant or lipid distribution, the centre of the bilayer is expected to lie on an infinite periodic minimal surface (IPMS) [11]. In cubic phases of normal curvature, the IPMS lines the mid-surface of the water film (Fig. 1). Bicontinuous cubic phases are believed to be well-described by IPMS of cubic symmetry. Bicontinuous phases of other symmetries are also geometrically feasible, although their existence in liquid crystals has yet to be established.

The structure of an ordered bicontinuous mesophase is specified in general by two labels which distinguish the IPMS: its space group *symmetry* and its *topology*. For example, a number of possible bicontinuous morphologies arise within the space group, Im3m (#229), including bilayers draped over the P-surface, the I-WP surface or the Neovius (C(P)) surface [12]. All three structures have been conjectured to occur in various liquid crystalline mesophases [13]. In principle, the symmetry of a crystalline mesophase can be directly determined from diffraction experiments (although the dynamics of these phases often result in poorly resolved diffraction spectra). The topology of the phase, which characterizes the connectivity of the tunnel network of the bicontinuous morphology, is less readily deduced. The topology of the bilayer is conventionally described by the genus, g, or its Euler- Poincaré characteristic, χ, per unit cell of the underlying IPMS. (These indices are linked *via* the relation valid for orientable surfaces, $\chi = 2 - 2g$).

A number of techniques for deducing the genus per unit cell of the bilayer have been published previously; all require knowledge of the chain length of the surfactant molecules, the unit cell

dimensions and the composition of the mixture and some require values of the head-group area [11, 14, 15]. These techniques assume that the polar-apolar interfaces in the aggregate form parallel surfaces to an IPMS. The parallel surface approach is used throughout this paper also The "master plot" technique has been shown to provide useful topological information, provided that the bilayer thickness and head-group area (which allows the monolayer area per unit cell, A, to be determined) can be independently estimated. These estimates are usually made by assuming their values are close to those in neighbouring phases, such as lamellar and hexagonal phases. If the morphology of the bilayer - its topology and symmetry - remain fixed during swelling, a plot of $2\pi l^2/a^2$ *vs.* $A/(2a^2)$ (a is the lattice parameter of the crystal) is linear, with slope χ, and intercept σ, characteristic of the bicontinuous morphology [3, 19]. It is clearly preferable to be able to determine the bilayer topology without resorting to such *ad hoc* assumptions. In fact, the technique can be improved.

In the next section, we show how the topology can be estimated without prior knowledge of the head-group area, although the bilayer thickness (twice the monolayer width, l) must be known. Following that, we demonstrate that the functional form of the bilayer swelling is sensitive to the location (if any) of an inextensible "neutral" surface (equivalent to the "pivotal" surface described in [16]), and a more accurate analysis of swelling is derived.

The Swelling of Normal and Reversed Hyperbolic Bilayers

Imagine a folded bilayer (of reversed curvature, i.e. enclosing water channels) whose mid-surface lies on an IPMS. This surface has zero mean curvature and non-positive Gaussian curvature at all points, i.e. it is equally curved towards both intertwined sub-volumes ([1]). An average measure of the bilayer curvature is afforded by the average Gaussian curvature,

$$< K >= \frac{\int_W K \mathrm{d}_a}{A(W)}$$

where $A(W)$ is the surface area of the region W of the surface. In crystalline mesophases, W typically refers to an integral multiple of the asymmetric patch of the IPMS, such as a unit cell. In disordered mesophases, W refers to a volume of the assembly which is at least as large as the cube of a characteristic distance of the mesostructure, such as the average spacing between bilayers. This average Gaussian curvature is related to the average magnitude of the radii of curvature, $< R >$, by the equation $< R >=< -K >^{-1/2}$

The volume of space $V(x)$ bounded by a saddle-shaped patch, W, of the IPMS of area A_0, the parallel surface to W displaced from the IPMS by a distance x and the surface normals around the boundary of W is [11]:

$$V(x) = A_0 x \left(1 - \frac{x^2}{3 < R >^2}\right) \tag{1}$$

Consider now a film of half-thickness x, whose mid-surface lies on an IPMS. The film volume is $2V(x)$. We assume that the film is "homogeneous", i.e. its Gaussian curvature is nearly constant In this case, the volume of space associated with the region W of the film is bounded by the pencil of normal vectors around the boundary of W, pointing towards both sides of the

([1]) By analogy with a planar curve, a surface is characterized by two radii of curvature, whose reciprocals are the principal curvatures, k_1 and k_2. The mean (M) and Gaussian (K) curvatures are defined by $M = (k_1 + k_2)/2$ and $K = k_1 \cdot k_2$

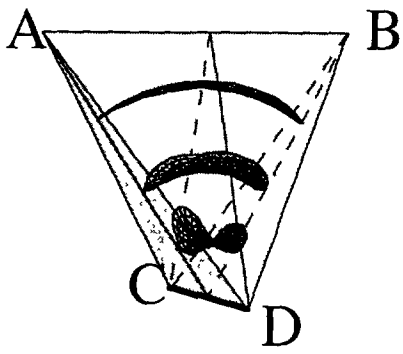

Fig. 2. — Schematic picture of the tetrahedron which defines the volume of space associated with a minimal surface patch, shown in the centre of the tetrahedron. The edges AB and CD define the location of tunnel axes on either side of the surface

film, which is a tetrahedron (Fig. 2) whose two edges AB and CD define the axes of the tunnels in the IPMS. Each tunnel axis lies at a distance equal to the average radius of curvature, $< R >$ from the mid-surface. From equation (1), the half-volume of the tetrahedron is:

$$V_{1/2} = A_0 < R > \left(1 - \frac{< R >^2}{3 < R >^2}\right) = \frac{2A_0 < R >}{3} \tag{2}$$

The volume fraction of the film, $\Phi_x = \dfrac{V(x)}{V_{1/2}}$ is thus:

$$\Phi_x = \frac{3\left(\dfrac{< R >}{x}\right)^2 - 1}{2\left(\dfrac{< R >}{x}\right)^3} \tag{3}$$

The scaled average radius of curvature of the homogeneous film (measured at the mid-surface of the film) as a function of the "concentration" of the film is thus:

$$\left[\frac{x}{< R >}\right] = -\cos\left(\frac{\Delta}{3}\right) + \sqrt{3}\sin\left(\frac{\Delta}{3}\right), \quad \text{where} \quad \Delta \equiv \tan^{-1}\left(\frac{\sqrt{1-\Phi_x^2}}{-\Phi_x}\right) \tag{4}$$

These equations are directly applicable to lyotropic bicontinuous mesophases, where the film may be the water layer or the bilayer (of half-thickness x). Assume for convenience that the mesophase is crystalline. The required relation between the lattice parameter and the topology of the bicontinuous phase (per crystallographic unit cell) emerges by way of a dimensionless constant, known as the "homogeneity index", H, which links the surface area of the IPMS per unit cell, A_{uc}, the volume of the unit cell, V_{uc}, and the Euler-Poincaré characteristic per unit cell, χ [17]:

$$H \equiv \frac{A_{uc}^{3/2}}{(2\pi\chi)^{1/2}V_{uc}} \approx \frac{3}{4} \tag{5}$$

(The value of 3/4 has been derived analytically for ideal homogeneous minimal surfaces. The exact value of H *depends* on the IPMS, but for low-genus IPMS which typically occur in bicontinuous mesophases, the approximation is a good one, c.f. Tab. I.)

Table I. — *Symmetry, Euler-characteristic (χ), genus per conventional cubic unit cell and homogeneity index for various IPMS.*

IPMS	*space group symmetry*	χ	*genus*	*H*
gyroid	Ia3d	-8	5	0 .7665
P-surface	Im3m	-4	3	0.7163
D-surface	Pn3m	-2	2	0.7498
I-WP surface	Im3m	-6	4	0.7425
Neovius (C(P))	Im3m	-16	9	0.6640

The area of the mid-surface of the film, A_{uc}, is related to the average Gaussian curvature of the mid-surface *via* the standard equality $< K > A_{uc} = 2\pi\chi$, which implies that $A_{uc} = -2\pi\chi < R >^2$.

Combining this with equation (5) gives:

$$\chi = \frac{-H}{2\pi}\left(\frac{\alpha}{< R >}\right)^3 \tag{6}$$

where $\alpha \equiv V_{uc}^{1/3}$ (e.g. the lattice parameter of cubic phases).

Consider first bilayers of reversed curvature (e.g. V_2 phases). Assume that the bilayer consists of identical back-to-back monolayers, in which case the mid-surface of the bilayer defines a minimal surface. The required equation for the bilayer topology in terms of the lattice parameter, α, the composition, Φ, and monolayer thickness, l, follows from (4) and (6):

$$\chi = \frac{-H}{2\pi}\left(\frac{\alpha}{l}\left(-\cos\left(\frac{\Delta}{3}\right) + \sqrt{3}\sin\left(\frac{\Delta}{3}\right)\right)\right)^3 \tag{7}$$

The lattice parameter is expected to vary with the surfactant concentration according to the formula:

$$\begin{aligned}\left[\frac{\alpha}{l}\right] &= \left(\frac{-2\pi\chi}{H}\right)^{1/3}\left(\sqrt{3}\sin\left(\frac{\Delta}{3}\right) - \cos\left(\frac{\Delta}{3}\right)\right)^{-1} \\ &\approx \left(\frac{-8\pi\chi}{3}\right)^{1/3}\left(\sqrt{3}\sin\left(\frac{\Delta}{3}\right) - \cos\left(\frac{\Delta}{3}\right)\right)^{-1}\end{aligned} \tag{8}$$

assuming that the minimal surface is homogeneous.

The analogous relations for bicontinuous mesophases of normal curvature (such as V_1 phases) are as follows. Here, the IPMS runs through the mid-surface of the water film, and the lipophilic moieties form interpenetrating fenestrated channels on either side of the polar film. If the half-thickness of the water film is t, the volume fraction of water, $\Phi_w = \frac{V(t)}{V_{1/2}}$, is given by the expression:

$$\Phi_w = \frac{t\left(3 - \left(\frac{t}{< R >}\right)^2\right)}{2 < R >}$$

(from (1) and (2)).

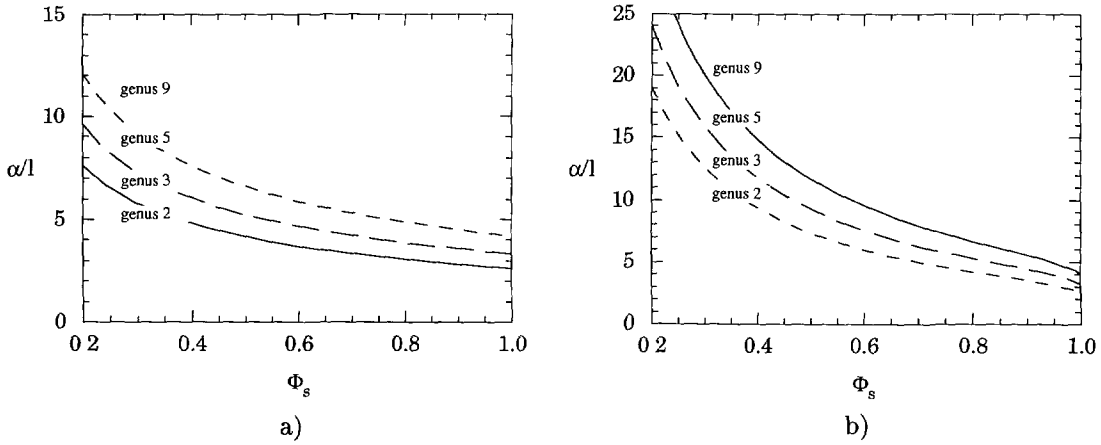

Fig 3 — Variation of the scaled lattice parameter with composition for bicontinuous cubic (V_1 (a); V_2 (b)) mesophases of different genera per unit cell, from equations (11) and (8) in the main text. (α is the "lattice parameter" of the mesophase, equal to the cube root of the unit cell volume, l is the width of the monolayer and Φ_s is the lipid/surfactant volume fraction.).

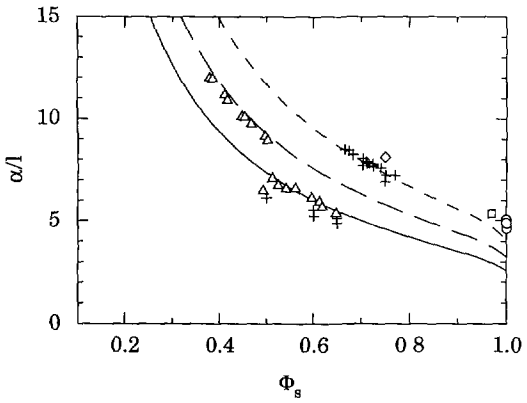

Fig. 4. — Plot of experimental data points for some bicontinuous reversed cubic phases (V_2), together with theoretical swelling curves for genus two structures (full curve), genus three (long-dashed curve) and genus five (short-dashed curve), from equation (8) in the main text. Crosses represent data for the (room temp) glycerol monooleate - water system, (l = 17 Å; data from [1, 18]; this paper). Delta symbols denote data from the pseudo-binary didodecyl dimethyl ammonium bromide - water - cyclohexane cubic phases (l = 13 Å[19]); the diamond denotes a sample within the AOT - water cubic phase (l = 7 Å[20]) The square denotes data for the high temperature lecithin - water cubic phase (l = 18 Å[21]) and the circles denote high temperature strontium carboxylate soaps (SrC_{12}: l = 12.6 Å, SrC_{14}· l = 12.4 Å; SrC_{16}, l = 13.1 Å; SrC_{18}: l = 14 3 Å; SrC_{20}, l = 15.0 Å. The C_{14} and C_{18} molecular lengths have been estimated from the neighbouring H_2 phase, and the others estimated from data for the corresponding Ca soaps [22]).

If $\gamma \equiv \dfrac{t}{< R >}$, one has

$$3\gamma - \gamma^3 = 2\Phi_w \tag{9}$$

Since $< R >= l + t$, equation (6) implies:

$$\chi = \frac{-H}{2\pi}\left(\frac{\alpha}{l}\right)^3 (1-\gamma)^3 \tag{10}$$

The swelling functional of a bicontinuous phase of direct morphology is thus:

$$\frac{\alpha}{l} = \left(\frac{-2\pi\chi}{H}\right)^{1/3}\left(\frac{1}{1-\gamma}\right) \approx \left(\frac{-8\pi\chi}{3}\right)^{1/3}\left(\frac{1}{1-\gamma}\right) \tag{11}$$

where γ is the single physically accessible root of the cubic polynomial (9).

Plots of the expected swelling as a function of the bilayer topology for both direct and reversed phases are illustrated in Figure 3.

These theoretical curves are readily generalizable to bilayers whose mid-surface does not define a minimal surface. (To lowest order, this generalization can be made by simply inserting the relevant value of H into Eqs. (8) and (11)). The equations agree well with measured lattice spacings in some bicontinuous cubic mesophases of lyotropic liquid crystals. It is clear from Figure 4 that over a wide range of concentrations and temperatures the measured dimensions of the cubic mesophases agree with the values expected from the swelling equations above. Clearly, the structural assignments of the V_2 phases, *viz.* the gyroid, the P-surface and the D-surface, are topologically correct. Further, the assumed value for H (ca. 3/4) is also in agreement with the data, so that it is reasonable to claim that these bilayers wrap onto IPMS.

Logarithmic Swelling Laws

These swelling equations can be best compared with the expected swelling behaviour of other morphologies, including sheet-like (lamellar) aggregates and globular and rod-like micellar aggregates, using log-log plots of the lattice parameter *vs.* composition. (The swelling laws for lamellar, spherical and cylindrical aggregates are outlined in the Appendix.) It is clear from Figure 5 that logarithmic plots offer a useful technique for characterizing the morphology of aggregates in direct phases. The differences between reversed mesophase morphologies are less marked, except for highly concentrated mesophases.

There is a remarkable similarity between the slopes of these plots and an index of the local molecular shape within the aggregates, known as the surfactant parameter [23]. This shape parameter is dependent on the curvatures of the interface. It is defined to be equal to v/al, where v is the volume bounded by a patch on the interface and a parallel surface to the patch, a is the area of the patch and l is the separation between the parallel surface and the patch. Consider the variation of this volume $v(\xi)$, as a function of the separation distance, ξ, the area of the patch, $a(\xi)$ and the (variable) surfactant parameter, $s(\xi)$. This volume variation is equal to the area, so that:

Since $s(\xi) = \dfrac{v(\xi)}{a(\xi)\xi}$,

$$v'(\xi) = a(\xi) = s'(\xi)a(\xi)\xi + s(\xi)a'(\xi)\xi + s(\xi)a(\xi) \tag{12}$$

where the prime denotes a partial derivative with respect to ξ.

This equation can be integrated to give:

$$a(\xi) = c\,\xi^{-1}\exp\left(\int \frac{s' - 1(\xi)\xi}{s(\xi)\xi}\mathrm{d}\xi\right) \tag{13}$$

where c is a constant.

If the surfactant parameter remains constant (s) as ξ is varied, so that the shape of the aggregate is fixed, we obtain the area scaling equation:

$$a(\xi) = c\,\xi^{1-s/s} \tag{14}$$

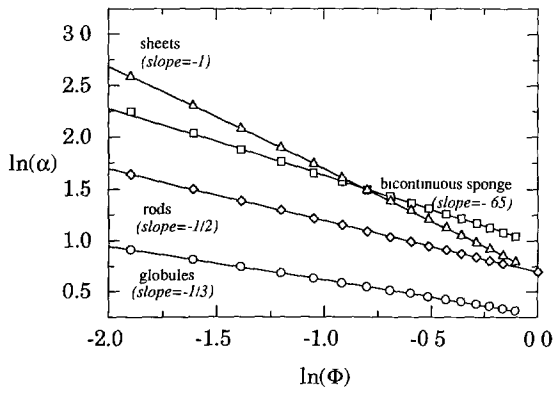

a)

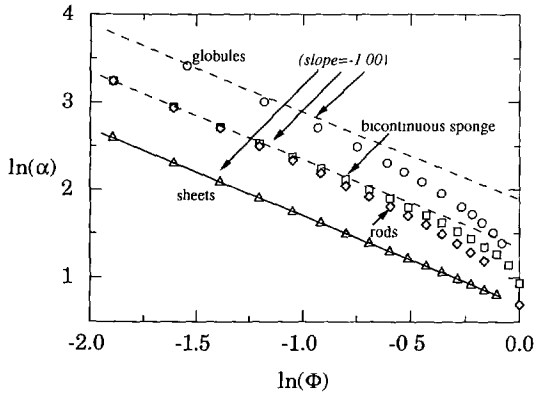

b)

Fig. 5 — Logarithmic plots of the volume fraction of surfactant/lipid (Φ) *vs.* characteristic spacing (α), for binary direct (upper) and reversed phases (lower) of globular (e g I_1, I_2 resp.), rod-like (H_1, H_2), sheet-like (L_α) and bicontinuous sponge (V_1, V_2, L_3) morphologies from equation (11) derived in the main text and the equations in the Appendix. These formulae are derived under the assumption that the width of the molecular monolayers is independent of the concentration of the fluid mixture. The gradients of these plots are universal for the various morphologies and are independent of the symmetry of the mesophases and the genus of the sponge morphology (both of which determine the value of the intercept). If the mesophase swells inhomogeneously, for example by variation of the *c/a* tetragonality ratio within a tetragonal phase, the spacing α is defined to be equal to $V^{1/3}$, where V is the volume per unit cell.

The constant, c, can be determined as follows. Two characteristic lengths in the system are the *intra*-aggregate radius, l, and the *inter*-aggregate (half) spacing, α. If the aggregate is a hyperbolic bilayer, l is equal to the half-thickness of the bilayer and α is equal to $- < K >^{-1/2}$. If the aggregate is a hyperbolic monolayer, carving out a porous network in the solvent, l is equal to the pore radius and α is equal to the average spacing between pores. If the sliding length parameter, ξ, is set to α, the area is $a(\alpha)$, so that

$$c = \frac{a(\alpha)}{\alpha^{(1-s)/s}} \tag{15}$$

The volume fraction of the aggregate for a film of thickness l, Φ, is then related to the surfactant parameter within the aggregate, s and the "surfactant parameter" for the parallel surface to the interface between the solvent and the film, located at the distance α, s_α:

$$\Phi = \frac{sa(\xi)\xi}{s_\alpha a(\alpha)\alpha} = \frac{s}{s_\alpha}\left(\frac{l}{\alpha}\right)^{1/s} \tag{16}$$

Thus, the characteristic spacing, α, is expected to scale with the composition like:

$$\log(\alpha) \sim -s\log(\Phi) \tag{17}$$

provided the variation of the surfactant parameter remains small and the aggregate "thickness", l, remains constant. The surfactant parameter is exactly constant, with respect to ξ variations, if the aggregates are spherical (oil-in-water, $s = 1/3$), cylindrical (oil-in-water, $s = 1/2$) or lamellar ($s = 1$). In other cases, $s'(\xi)$ is not zero.

The gradients of these log-log plots are valid for a given morphology, and hold for both crystalline and disordered mesophases. In both cases α denotes any characteristic length scale in the mesostructure. In order for the scaling laws to be applicable the film thickness must remain constant and the topology, χ (e.g. per unit cell for crystals, per unit volume (α^3) for disordered phases) of the film must remain fixed during dilution or concentration of the phase. Further, the homogeneity index, H, of the film must remain constant, which generally implies that the mean curvature of the film does not vary during the swelling. (H depends on the symmetry and topology of the structure, however, this effect is a minor one, particularly for low-genus surfaces, c.f. Tab. I.)

This swelling analysis is useful, although it is less than the whole story. So far, we have focused on mesophase swelling which preserves the film thickness. Other swelling modes are possible, which allow for the thickness to vary on swelling. In particular, we focus on transformations which conserve the area of a parallel surface to the mid-surface of the film. We call this the "neutral" surface.

The existence of a neutral surface is a result of central importance to understanding the stability of both lyotropic and thermotropic mesophases, since the neutral surface (or the "pivotal surface") is the simplest location at which to locate an imaginary surface that describes the film bending energy [16]. The location of the neutral surface determines the relative stability of bicontinuous geometries, and the whole approach adopted in this area to data - modelling films by imaginary surfaces - relies on as-yet unproven assumptions about the nature and existence of this surface.

Neutral Surfaces in Crystalline Bicontinuous Mesophases of Reversed Curvature

The swelling behaviour of bilayers of reversed curvature can be readily analyzed assuming the neutral surface is a parallel surface displaced from the mid-surface of the bilayer by a distance t. The homogeneity index of the mid-surface of the film (assumed to be a minimal surface) is:

$$H \equiv \frac{A_{\mathrm{uc}}^{3/2}}{(-2\pi\chi)^{1/2}\alpha^3} = \frac{\left(\frac{n_{\mathrm{s}}\Omega(0)}{2}\right)^{3/2}}{(-2\pi\chi)^{1/2}\alpha^3} \tag{18}$$

where $\Omega(0)$ is the area per surfactant molecule at the mid-surface of the film, and n_{s} denotes the number of surfactant molecules per unit cell of the film. The volume fraction of the film,

$$\Phi = \frac{n_{\mathrm{s}}\nu_{\mathrm{s}}}{\alpha^3} \tag{19}$$

where ν_s is the volume of a surfactant molecule.

Combining (18) and (19) gives:

$$\Omega(0) = \frac{2\nu_s(-2\pi\chi H^2)^{1/3}}{\alpha\Phi} \tag{20}$$

The area per surfactant molecule at the parallel surface to a periodic minimal surface is:

$$\Omega(t) = \Omega(0)\left(1 + \frac{2\pi\chi t^2}{A_{uc}}\right) \tag{21}$$

Combining (20) and (21) gives:

$$\Phi = \frac{\nu_s(-16\pi\chi H^2)^{1/3}\left(1 - \left(\left(\frac{2\pi\chi}{H}\right)^{1/3}\frac{t}{\alpha}\right)^2\right)}{\alpha\Omega(t)} \tag{22}$$

The swelling behaviour follows directly from this equation, once the location of the neutral surface (t) is set. For a reversed bilayer, we expect the position of this neutral surface to lie somewhere between $t = 0$ and one of the centres of curvature of the bilayer, $t =< R >$. The upper bound on t is related to the bilayer topology as follows. Since

$$A_{uc} = (-2\pi\chi H^2)^{1/3}\alpha^2 \quad \text{and} \quad A_{uc} = -2\pi\chi < R >^2$$
$$\frac{t}{\alpha} < \frac{< R >}{\alpha} = \left(\frac{H}{-2\pi\chi}\right)^{1/3} \tag{23}$$

The simplest swelling law follows if the neutral surface is located at the mid-surface of the bilayer ($t = 0$). In this case, characteristic lengths of the mesophase vary linearly with the inverse concentration of the film, $\alpha \sim \Phi^{-1}$. This form is identical to that for lamellar phases, and has (mistakenly) been widely used as a characteristic solely of a phase containing a stack of flat sheet-like aggregates.

If there is a neutral surface located within each hydrophobic chain region of the mesophase, at a fixed distance from the free chain ends towards the polar regions, t, the swelling as a function of reciprocal concentration is non-linear, particularly in concentrated systems. In this case, we rewrite the swelling equation (22):

$$\Phi = 4\pi\chi\left(\frac{\lambda}{\alpha}\right)^3\left(\left(\frac{t}{\lambda}\right)^2 - \left(\frac{H}{-2\pi\chi}\right)^{2/3}\left(\frac{\alpha}{\lambda}\right)^2\right), \qquad \lambda \equiv \frac{\nu_s}{\Omega(t)} \tag{24}$$

Provided the concentration is not too high, $\lambda \approx l$, since $\frac{\nu_s}{\Omega(t)l} \approx \frac{\nu_s}{\Omega(0)l} \approx 1$ so that $0 \leq t/\lambda \leq 1$ spans possible locations of neutral surfaces *within* each monolayer. As t/λ approaches unity, the α *vs.* Φ^{-1} function (Eq. (24)) exhibits increasing non-linearity. The range (of Φ^{-1}) of the single physically realistic branch of the function narrows, so that the formation of bicontinuous bilayers of reversed curvature is impossible above a maximum concentration, set by the exact location of the neutral surface (Fig. 6).

It turns out that the functional form of the swelling law assuming fixed film thickness is close to that due to a neutral surface located at $t/\lambda = 1/2$ (Fig. 6). Note, however, that it is impossible for the film thickness to remain exactly constant while maintaining a neutral surface at a constant distance from the mid-surface of the bilayer.

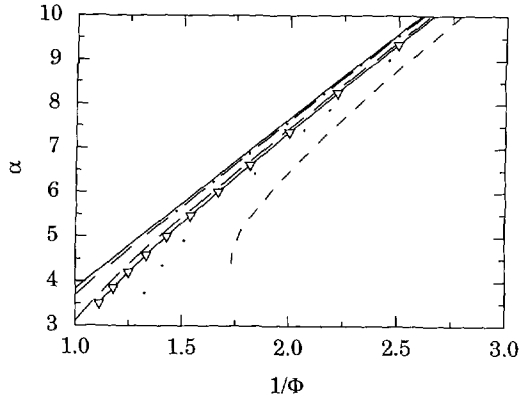

Fig. 6. — Plot of swelling (α is an arbitrary length scale in the structure) as a function of the volume fraction of the bilayer for hyperbolic bilayers of reversed curvature (e g V_2 phases, connected sponges), from equation (24) in the main text. The unmarked curves denote swelling laws assuming that the bilayer swells while maintaining a neutral surface located at a parallel surface to the mid-surface of the bilayer (i) approximately at the mid-surface of the bilayer (full line), (ii) approximately 1/4 of the way along the molecule $t/\lambda = 1/4$ (dotted-dashed curve) (iii) approximately 1/2 way along the molecule (large-dashed curve) (iv) approximately 3/4 along the molecule (dotted curve) (v) approximately at the water interface (small-dashed curve) The curve marked with open nablas denotes the swelling behaviour assuming the thickness of the bilayer remains constant.

In order to investigate the possibility of neutral surfaces in swelling mesophases, we have analyzed swelling data collected here and elsewhere for glycerol monooleate (GMO)-water mixtures within the two reported bicontinuous cubic phases [1, 18], as well as data within the cubic phase region of the DDAB - water - cyclohexane system [19]. If a neutral surface is maintained during swelling, whose location is fixed at a certain distance t from the mid-surface of the bilayer, the swelling data follows the polynomial derived from equation (24):

$$\Phi = c_1 \alpha^{-1} + c_2 \alpha^{-3},$$

where

$$c_1 = \frac{(-16\pi\chi H^2)^{1/3}\nu_s}{\Omega(t)} \qquad \text{and} \qquad c_1 = \frac{-4\pi\chi\nu_s t^2}{\Omega(t)} \tag{25}$$

Both linear ($c_2 = 0$) and cubic fits ($c_1, c_2 \neq 0$) have been determined numerically for bicontinuous cubic phases of GMO-water and DDAB-cyclohexane-water mixtures (Figs. 7-11).

The room temperature GMO-water data are consistent with a neutral surface located at the mid-surface of the GMO bilayer within both the Ia3d and Pn3m bicontinuous cubic phases (Figs. 7, 8). In other words, during swelling, both the thickness of the bilayer and the area per GMO molecule at the polar-apolar interface vary to maintain constant area per GMO at the IPMS. Further, within experimental uncertainty, the area per GMO molecule at the mid-surface is constant within both phases.

The data collected within the Ia3d phase also fit a model assuming neutral surfaces slightly displaced from the mid-surface, although the trend is not certain (Fig. 7). Given the uncertainty of the data, it is impossible to choose unequivocally one of these models over the other It is apparent from these plots that the exact location of the neutral surface(s) cannot be decided without more accurate data.

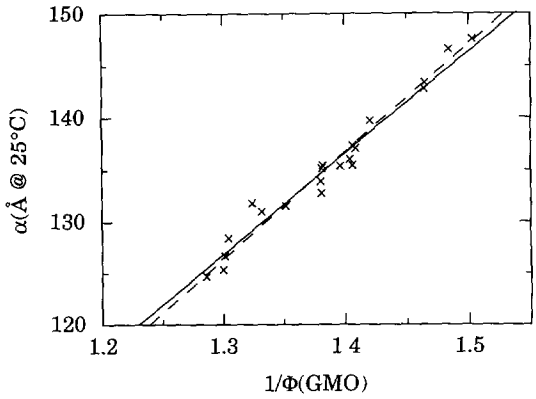

Fig. 7. — Swelling plot within the Ia3d bicontinuous cubic phase region of glycerol monooleate (GMO) - water mixtures at 25 °C, from equation (25). (Data courtesy of Chung and Caffrey. The lipid volume is taken to be 593 Å^3, corresponding to a density of 1g cm^{-3}) The full line is the best fit to the data assuming a constant area per GMO molecule at the mid-surface of the bilayer (37.0 Å^2). The dashed line indicates the best fit to the data assuming the area per GMO at the mid-surface varies with composition and the neutral surface lies towards the polar region within each monolayer (t = 5.5 Å, area per GMO at the neutral surface, 36.0 Å^2).

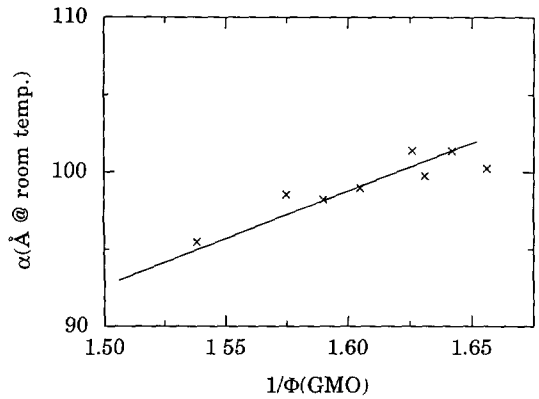

Fig. 8. — Swelling plot within the Pn3m bicontinuous cubic phase region of glycerol monooleate (GMO) - water mixtures at room temperature. (The lipid volume is taken to be 593 Å^3, corresponding to a density of 1g cm^{-3}) The full line is the best fit to the data assuming a constant area per GMO molecule at the mid-surface of the bilayer (36.9 Å^2), from equation (25). No physically realistic value for the location of a neutral surface displaced from the mid-surface can be deduced from this data (a best fit leads gives imaginary value for the distance, t).

The underlying physics of swelling of the bicontinuous Ia3d GMO-water phase at 35 °C is more clearly discernible. In this higher temperature mesophase, a model assuming the presence of neutral surfaces within each monolayer, approximately half-way along the GMO molecules, fits the data well, while one assuming a neutral surface at the mid-surface leads to a poor fit to the data (Fig 9). It is curious to note that the effect of elevating the temperature has been simply to shift the neutral surface towards the polar regions, without altering its area. Note however, that the data are also consistent with an assumed swelling at constant bilayer thickness (c.f. Fig. 6).

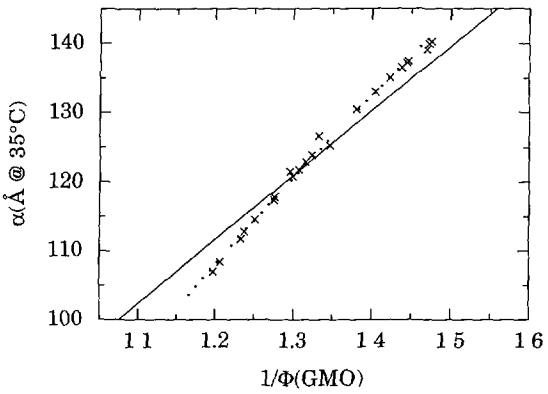

Fig 9. — Swelling plot within the Ia3d bicontinuous cubic phase region of GMO - water mixtures at 35 °C (Data courtesy of Chung and Caffrey.) The full line is the best fit to the data assuming a constant area per GMO molecule at the mid-surface of the bilayer (38.8 $Å^2$, assuming the molecular volume of GMO is 593 $Å^3$). The dotted line indicates the best fit to the data assuming the area per GMO at the mid-surface varies with composition and the neutral surface lies towards the polar region within each monolayer (t = 9.6 Å, where the area per GMO at the neutral surface is 34.8 $Å^2$), from equation (25).

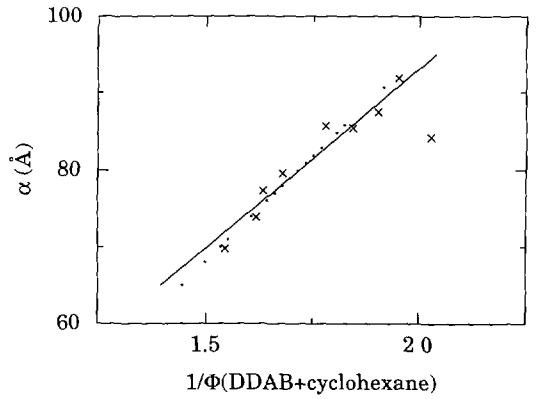

Fig 10. — Swelling plot within the Pn3m bicontinuous cubic phase region of DDAB - cyclohexane - water mixtures at room temperature. The full line is the best fit to the data assuming a constant area per DDAB molecule at the mid-surface of the bilayer (79.5 $Å^2$, volume of DDAB + cyclohexane per DDAB molecule equal to 1000 $Å^3$). The dotted line indicates the best fit to the data assuming the area per DDAB at the mid-surface varies with composition and the neutral surface lies towards the polar region within each monolayer (t = 6.1 Å, where the area per DDAB is fixed at 76.5 $Å^2$), from equation (25)

In both cubic mesophases of the DDAB system, the data are consistent with an inextensible mid-surface of the bilayer, viz. $t = 0$ (Figs. 10, 11). (There are slight indications of non-linearity, however, they remain at this stage inconclusive.) The area per surfactant molecule at the mid-surface is almost equal in both mesophases, as in the room temperature GMO-water system. Appropriate scaling (by the topology and homogeneity index) for each phase leads to a unified picture of the swelling across the entire domain of bicontinuous cubic phases. The scaled data for the DDAB system is plotted in Figure 12.

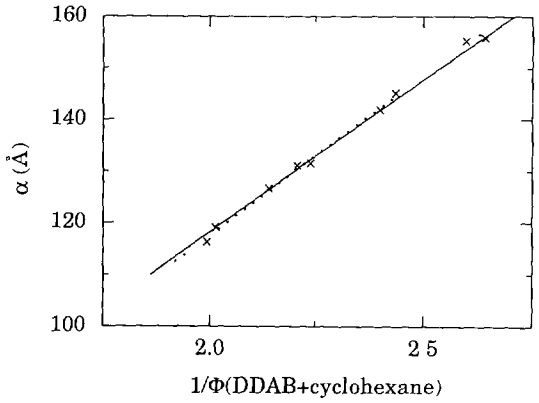

Fig. 11. — Swelling plot within the Im3m bicontinuous cubic phase region of DDAB - cyclohexane - water mixtures. The full line is the best fit to the data assuming a constant area per DDAB molecule at the mid-surface of the bilayer (area = 77 0 Å^2). The dotted line indicates the best fit to the data assuming the area per DDAB at the mid-surface varies with composition and the neutral surface lies towards the polar region within each monolayer (t = 7.9 Å, where the area per DDAB is fixed at 74 1 Å^2), from equation (25).

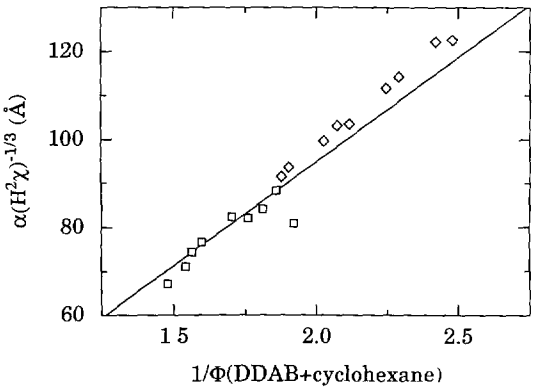

Fig. 12. — Swelling plot for both bicontinuous cubic phases detected in the DDAB - cyclohexane - water system. The diamonds and squares indicate data points in the Im3m and Pn3m cubic phases respectively The lattice parameter data (α) are normalized *via* the factor $(-H^2\chi)^{-1/3}$ to allow a direct comparison of the area per DDAB molecule at the free chain ends (the mid-surface of the bilayer) The linearity of the plot of normalised lattice parameter *vs.* hydrophobic volume fraction ($1/\Phi$) indicates that the area at the mid-surface of the bilayer is fixed throughout both cubic phases. The line of best fit leads to an area of 77.7 Å^2 per surfactant molecule at the mid-surface, from equation (28)

Crystalline Bicontinuous Mesophases of Normal Curvature

The formulae derived in the previous section are directly applicable to crystalline bicontinuous mesophases whose channels are lined with the lipophilic moiety (e.g. V_1 phases). In these cases however, the locations of the neutral surfaces (t) are close to $t =< R >$, rather than at the mid-surface of the (reversed) bilayer, $t = 0$. This difference accounts for the very different exponents of the swelling laws for normal and reversed bicontinuous phases, shown in Figure 5.

Disordered "Sponge" Phases

Some disordered mesostructured phases - called L_3 phases - exhibit flow birefringence. This defining characteristic probably disguises a multitude of mesostructures, based on molten columnar, globular (e.g. vesicular), lamellar or bicontinuous morphologies. The swelling formulae derived so far are also applicable to these cases, and they may be used to determine the morphology of the aggregates within an L_3 phase. Scattering spectra of L_3 phases typically exhibit a single broad peak, whose location in reciprocal space is related to the inverse of a characteristic spacing within the mesostructure in real space. This spacing can be used in place of the lattice spacing typical of crystalline mesophases, in order to study swelling characteristics. The functional form of the swelling data can be used to determine the mesophase morphology, as well as the approximate location of a neutral surface within the mesophase. Note however, that in the absence of extra data (such as the bilayer thickness), absolute values of the neutral surface area and location cannot be deduced.

A water-rich "sponge" phase (denoted L_1^*, presumed to be of normal curvature and of sponge morphology) has been identified in mixtures of water-NaCl-pentanol and sodium dodecyl sulphate (SDS), and a related oil-rich (L_2^*, reversed curvature) sponge phase in water-dodecane-pentanol-SDS mixtures [10]. In the original study, the characteristic spacing (α) was found to vary approximately as $\alpha \sim \Phi^{-1}$ in both phases. This result is inconsistent with the swelling laws derived above (Fig. 5), since this implies that the aggregates are of reversed curvature (and any morphology!). Closer analysis of this data shows deviations from this swelling relation. Accordingly, we have reanalyzed the data, estimated from the original figure and listed in Table II.

The L_1^* data fit reasonably well within a sponge model (Fig. 13), provided the neutral surfaces are displaced from the mid-surface of the bilayer. From equation (25), the distance between the neutral surfaces and the mid-surface, t, is related to the topology of the bilayer

Table II. — *Estimates of the characteristic spacing vs. composition from Figure* 5 *of* [10].

Phase	Volume fraction of bilayer (F)	Characteristic spacing, α (Å)
L_1*	0.064	475
	0.087	330
	0.142	200
	0.231	125
	0.247	100
L_2*	0.054	535
	0.067	450
	0.091	320
	0.145	160
	0.185	135
	0.239	125

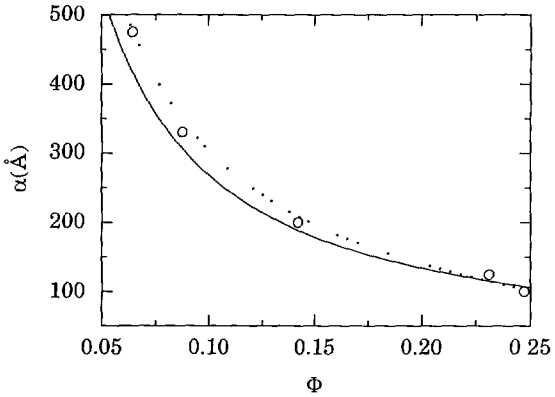

Fig. 13. — Reanalysis of swelling data within the L_1^* mesophase, recorded by Gazeau *et al.* (SDS-water-pentanol-NaCl mixtures [10]). The peak position in X-ray spectra is denoted by α. The full curve assumes that the area per SDS molecule at the mid-surface of the bilayer is independent of dilution (volume fraction of the bilayer = Φ), viz $\alpha \sim \Phi^{-1}$. The dotted curve assumes neutral surfaces displaced from the mid-surface, using equation (25), whose locations are discussed in the main text.

within a volume α^3 (where α is the characteristic spacing (Å), equal to the centre of the broad scattering peak - real space - detected within the phase), χ by the relation:

$$t = \left(\frac{H}{-2\pi\chi}\right)^{1/3} \left(\frac{c_2}{c_1}\right)^{1/2} \tag{26}$$

where c_1 and c_2 are determined by the best fit of the polynomial (25) to the swelling data.

For a symmetric sponge morphology, the mean curvature at the centre of the bilayer vanishes, so, assuming homogeneity, $H = 3/4$, and:

$$t \approx -0.5\chi^{-1/3} \left(\frac{c_2}{c_1}\right)^{1/2} \tag{27}$$

(Note that for very dilute bilayers, this homogeneity assumption may break down, given the large bilayer fluctuations associated with these phases) The data of Gazeau *et al.* within this mesophase are most accurately modelled by a polynomial fit of the following form:

$$\Phi = 30.99\alpha^{-1} - 57440\alpha^{-3}$$

so that the neutral surfaces are displaced by a distance of ca. $-21\chi^{-1/3}$Å. In the absence of independent knowledge of the relation of the peak position to the topology of the membrane, nothing more can be said. (This issue is discussed further in the following section.) Note however, that since χ is of the order of -1, the neutral surfaces are located about 20 Å away from the mid-surface of the bilayer, which is a reasonable value for a sponge phase of direct morphology.

The L_2^* data exhibit systematic deviations from the swelling behaviour expected for a sponge, regardless of the location of the neutral surface (Fig. 14). So far, however, we have assumed that the mean curvature at the centre of the bilayer vanishes (i.e. a symmetric sponge). The swelling equations are readily generalized to a case where the mean curvature at the mid-surface of the bilayer (normal or reversed) differs from zero (M), using the parallel surface equation

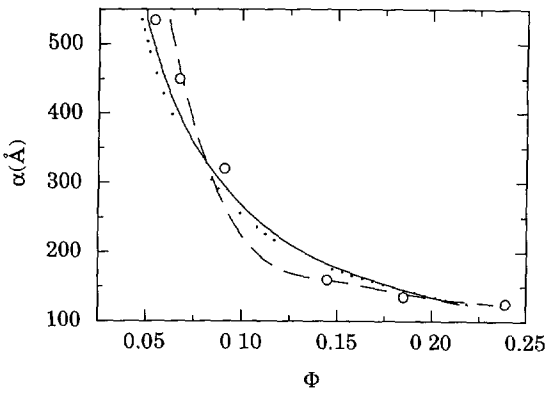

Fig. 14. — Swelling data (circles) for the L_2^* phase [10]. The full line indicates the best fit assuming a neutral surface at the mid-surface of the (assumed symmetric, sponge-like) bilayer The dotted line indicates the best fit assuming a symmetric sponge-like bilayer, from equation (25), whose neutral surfaces are displaced from the mid-surface. The dashed curve is a best fit, from equation (30), to the data assuming an asymmetric sponge-like bilayer, whose neutral surfaces are removed from the mid-surface.

analogous to equation (1):

$$V(x) = A_0 x \left(1 + Mx - \frac{x^2}{3 < R >^2}\right) \tag{28}$$

This leads to an additional term in the final swelling equation:

$$\Phi = \frac{\nu_s \left(-16\pi H^2 \chi\right)^{1/3} \left(1 + (M\alpha) t\alpha^{-1} - \left(\left(\frac{2\pi\chi}{H}\right)^{1/3} \frac{t}{\alpha}\right)^2\right)}{\alpha\Omega(t)} \tag{29}$$

(Note that the mean curvature is scaled by the characteristic distance, so that the variable $M\alpha$ is a measure of the asymmetry of the membrane.) The polynomial describing the swelling of an asymmetric bilayer is thus of the form:

$$\Phi = c_1\alpha^{-1} + c^2\alpha^{-2} + c_3\alpha^{-3} \tag{30}$$

The swelling data for this mesophase is reasonably well-described by a polynomial of this form. The scaled mean curvature, $M\alpha$, can be estimated from the coefficients of the polynomial *via* the equation:

$$M\alpha = H^{-1/3} c_1^{-1/2} c_2^{3/2} c_3^{-1} \tag{31}$$

and the location of the neutral surfaces by equation (27). Note that the value of the homogeneity index, H, is dependent on the mean curvature; it is of the order of unity. The best fit to the data assuming an asymmetric sponge-like bilayer,

$$\Phi = 24.14\alpha^{-1} + 2214\alpha^{-2} - 213770\alpha^{-3}$$

results in a scaled mean curvature of ca. 0.01, and a displacement from the mid-surface of $4.8\chi^{-1/3}$, which suggests that the mesophase is indeed a reversed phase (since the neutral surfaces lie ca. 4.8 Å from the bilayer centre).

A more conclusive analysis of these systems clearly requires further data. However, we hope that this preliminary analysis of some "sponge" data demonstrates that X- ray data in isolation does expose many structural features of these disordered systems.

Discussion

A number of swelling relations have been derived for bicontinuous bilayers in water, which we have modelled as single-sheeted hyperbolic films. We have focused here on the functional form of the swelling behaviour, since this approach avoids assumptions about bilayer dimensions. The functional form of the swelling depends on the details of the swelling mechanism. The simplest form results if the area of the mid-surface of the bilayer remains unchanged as the composition of the lyotropic mesophase varies. In this case, characteristic dimensions of the mesophase vary linearly with the reciprocal of the concentration, $\alpha \sim \Phi^{-1}$.

This result is not new: it was first suggested by Porte *et al.* [9] in their study of the scaling behaviour of random isotropic films. However, their result was derived from a simple "plaquette" approximation to the P-surface: its validity to smoothly curved surfaces of arbitrary topology remained unknown. It is apparent from equation (16) that this scaling behaviour is valid assuming (i) constant area per surfactant or lipid molecule at the mid-surface of the bilayer or (ii) low concentration.

According to Porte *et al.* the constant of proportionality is close to $3l$ (recall that l is the monolayer thickness); the linearised approximation to equation (16) (valid assuming (i) or (ii)) gives a constant of proportionality of

$$\frac{(-16\pi\chi H^2)^{1/3}\nu_s}{\Omega(t)}.$$

Provided condition (ii) is satisfied, $\frac{\nu_s}{\Omega(t)} \approx l$, so that

$$\alpha \approx \frac{(-16\pi\chi H^2)^{1/3} l}{\Phi} \tag{32}$$

If the bilayer mid-surface is a (homogeneous) minimal surface, $H = 3/4$, and the swelling law can be written as:

$$\alpha \sim -3.05\chi^{1/3}\Phi^{-1}$$

Porte *et al.* have assumed that the characteristic dimension, α, is a typical pore size, viz $(1/2)^3$ of the conventional (genus three) unit cell, so that $\chi = -1/2$, yielding a constant of 2.42. (The facetting of Porte's surface, which leads to a large area relative to a homogeneous surface, and thus a relatively large value of H, is responsible for the discrepancy between the scaling constants). It is evident from equation (32) that the scaling factor is dependent both on the topology of that portion of the film characterized by the dimension α, and the homogeneity index H, which is (to lowest order) dependent on the mean curvature of the mid-surface of the film.

In short, the "linear" functional form of the scaling behaviour (32) is a valid approximation below about 40% (v/v) lipid content, regardless of the location (if any) of the neutral surface(s). This functional form has been shown earlier to agree with swelling measurements of some disordered "symmetric sponge" (L_3) mesophases [9, 10]. We have shown here that a slightly more complex form can also be used to detect asymmetric sponges It is also a reasonable model for the room temperature GMO - water and the DDAB - cyclohexane - water cubic mesophases. In these crystalline systems, phase transitions between cubic mesophases apparently occur

without any significant change in the area of the IPMS describing the mid- surface of the bilayer. The coexisting bicontinuous mesophases which form at the (first order) transitions are thus well modelled by three isometric IPMS, the P- surface, the gyroid and the D-surface. These IPMS are related by the Bonnet transformation, which has been shown earlier to be a useful description of the D-surface - gyroid transition in the GMO-water system at room temperature [24]. Clearly, this transformation, which also links the D- and P-surfaces, is also a valid one within the DDAB - cyclohexane - water system. The swelling equations imply that for coexisting hyperbolic membranes related by the Bonnet transformation, the ratio of lattice parameters of the mesophases is:

$$\frac{\alpha_1}{\alpha_2} = \left(\frac{H_2^2\chi_2}{H_1^2\chi_1}\right)^{1/3} \tag{33}$$

The swelling behaviour departs from linearity - particularly in concentrated systems - once the neutral surface moves away from the mid-surface of the bilayer. This feature has been detected in a GMO - water cubic mesophase at 35 °C.

It should be noted that an accurate determination of the location of neutral surfaces requires data over a large span of compositions, since only then can the linearity or otherwise of the swelling function be established. This restricts the number of analytically accessible systems severely. However, in the future we hope to return to this issue to analyse the swelling behaviour of thermotropic mesophases, which remains unexplored.

Acknowledgments

We are very grateful to Martin Caffrey, Hesson Chung and Jason Briggs for providing us with their raw data, which inspired us to investigate this issue in detail. We also thank Vittorio Luzzati for stimulating discussions about bicontinuous mesophases.

Appendix

The swelling behaviour of "classical" aggregates, viz. spheres, cylinders and planes is easily derived from standard geometrical formulae relating volumes and radii. In all cases we adopt the assumption that the volume associated with an aggregate, or patch of an aggregate, is bounded by a surface that is parallel to the surface bounding the aggregate (which is the polar-apolar interface in surfactant-water aggregates). Two length scales are relevant. The first, l, describes the average half-width of the film, i.e. the aggregate radius or half-thickness. Further, the length α describes half the average spacing between the aggregates.

Consider first the case of spherical aggregates of direct morphology. In this case, the volume fraction of the aggregate in solution is:

$$\Phi = \left(\frac{l}{\alpha}\right)^3$$

Consider next spherical aggregates of reversed morphology (in which case the spheres are filled with the solvent). In this case, the volume fraction of the aggregate scales according to the law:

$$1 - \Phi = \left(\frac{\alpha - l}{\alpha}\right)^3$$

Similarly, for cylindrical aggregates of direct and reversed curvature, the scaling laws are:

$$\Phi = \left(\frac{l}{\alpha}\right)^2 \qquad \text{and} \qquad 1 - \Phi = \left(\frac{\alpha - l}{\alpha}\right)^2$$

respectively. For lamellar aggregates, the corresponding relations are:

$$\Phi = \left(\frac{l}{\alpha}\right) \qquad \text{and} \qquad 1 - \Phi = \left(\frac{\alpha - l}{\alpha}\right)$$

These equations allow the composition, Φ, to be related to the ratio α/l. The plots shown in Figure 5 follow directly.

A clue to the general scaling law given in equation (16) is already apparent. Notice that the exponents relating the composition to the ratio of the two length scales for spheres, cylinders and lamellae are 3, 2 and 1 respectively. The surfactant parameters (s) for (direct) aggregates of these morphologies are 1/3, 1/2 and 1/1 respectively, so that in these cases at least, the exponents are equal to $1/s$. This relation is in fact true for all morphologies; its general validity is derived in the main text.

References

[1] Chung H and Caffrey M., *Biophys. J* **66** (1994) 337

[2] Briggs J. and Caffrey M., *Biophys. J.* **66** (1994) 573-587.

[3] Maddaford P and Toprakiogliu C., *Langmuir* **9** (1993) 2868-2878.

[4] Chung H. and Caffrey M , *Nature* **368** (1994) 224-226.

[5] Fontell K., *Colloid Polym. Sci.* **268** (1990) 264-285.

[6] Larsson K , *J Phys Chem* **93** (1989) 7304-7314.

[7] Luzzati V , Vargas R , Mariani P., Gulik A. and Delacroix H., *J Mol Biol.* **229** (1993) 540-551.

[8] These phases were first mentioned by Krister Fontell, although they were only later named L_3 phases, see Fontell K., ACS Symposium Series, Colloidal Dispersion and Micellar Behaviour, (9) (1975) 270-277

[9] Porte G , Marignan J , Bassereau P and May R , *J Phys. France* **49** (1988) 511-519.

[10] Gazeau D., Bellocq A. M., Roux D. and Zemb T., *Europhys Lett* **9** (1989) 447-452.

[11] Hyde S. T , *J. Phys. Chem.* **93** (1989) 1458-1463;
see also Charvolin J., Sadoc J.-F., *J. Phys France* **48** (1987) 1559-1569.

[12] Andersson S , Hyde S. T , Larsson K. and Lidin S., *Chem. Rev* , **88** (1988) 221-242.

[13] Strom P. and Anderson D. M., *Langmuir* **8** (1992) 691-709.

[14] Barois P., Eidam D. and Hyde S. T., *J. Phys Colloq France* **51** (1990) C7-25-C7-34

[15] Turner D. C., Wang Z.-G., Gruner S. M., Mannock D A. and McElhaney R. N., *J. Phys. II France* **2** (1992) 2039.

[16] Kozlov M. M. and Winterhalter M., *J. Phys II France* **1** (1991) 1077.

[17] Hyde S T., Blum Z. and Ninham B. W., *Acta Cryst. A* **A49** (1993) 586-589.

[18] Lindblom G , Larsson K., Johansson L , Fontell K. and Forsen S , *J.A C S* **101** (1979) 5465-5470;
see also Larsson K. , *Nature* **304** (1983) 664;
Puvvada S , Qadri S. B., Naciri J and Ratna B. R , *J. Phys. Chem.* **97** (1993) 11103-11107.

[19] Barois P , Hyde S. T., Ninham B. W. and Dowling T., *Langmuir* **6** (1990) 1136-1140.

[20] Fontell K , *J Coll. Interf. Sci.* **43** (1973) 156-164.

[21] Reiss-Husson F , *J. Mol. Biol* **25** (1967) 363,
Luzzati V., Gulik-Krzywicki T. and Tardieu A., *Nature* **218** (1968) 1031-1034.

[22] Spegt P., Thèse, Université de Strasbourg (1964).

[23] Hyde S. T , *Pure Appl. Chem.* **64** (1992) 1617-1622 and references therein.

[24] Hyde S. T , Andersson S , Ericsson B and Larsson K , *Z. Kristallogr.* **168** (1984) 213-219.